Electronic Supplementary Information

Bromide-acetate co-mediated high power density rechargeable aqueous zinc-manganese dioxide batteries

Jing Wu[a,b], Yining Li[a,b], Jiaqi Huang[a,b], Xiaowei Chi[a], Jianhua Yang[a,b], Yu Liu[a*]*

Jing Wu, Yining Li, Prof. Xiaowei Chi, Prof. Jianhua Yang, Prof. Yu Liu

[a]Shanghai Institute of Ceramics, Chinese Academy of Sciences
Shanghai 200050, China
Email: xwchi@mail.sic.ac.cn
Email: yuliu@mail.sic.ac.cn
Jing Wu
[b]University of Chinese Academy of Sciences
Beijing 100049, China

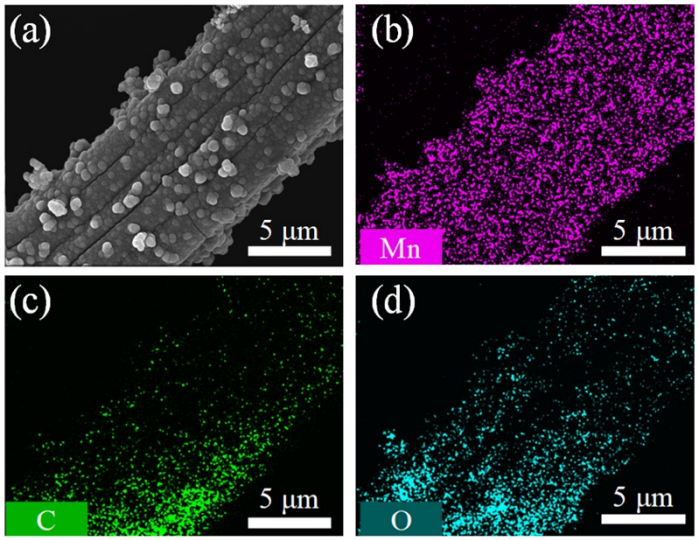

Figure S1. Elemental mapping distribution images of the electrodeposited MnO_2 on the carbon fibers substrate.

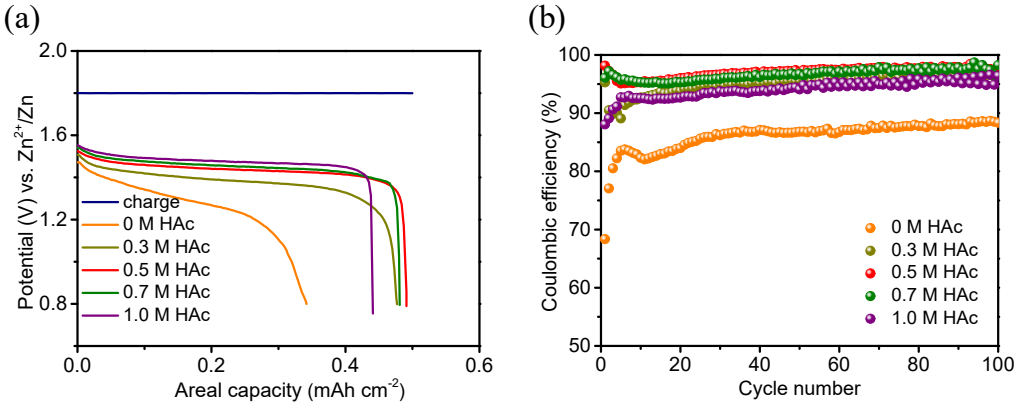

Figure S2. (a) Charge and discharge profiles and (b) cycling performance of acetate-based electrolyte with different concentrations of acetic acid (HAc) buffering agent at limited charge capacity of 0.5 mAh cm^{-2} and discharge current density of 1 mA cm^{-2}.

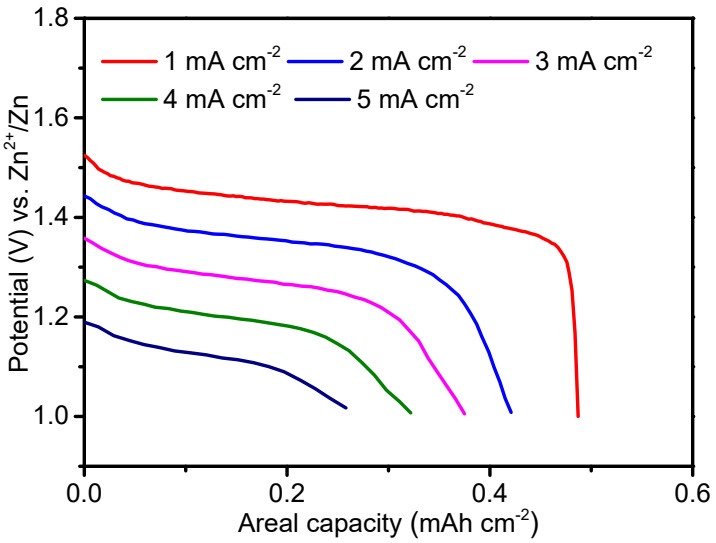

Figure S3. The discharge profiles of the Zn-MnO_2 battery at different discharge current densities from 1 to 5 mA cm^{-2} in the KBr-free electrolyte.

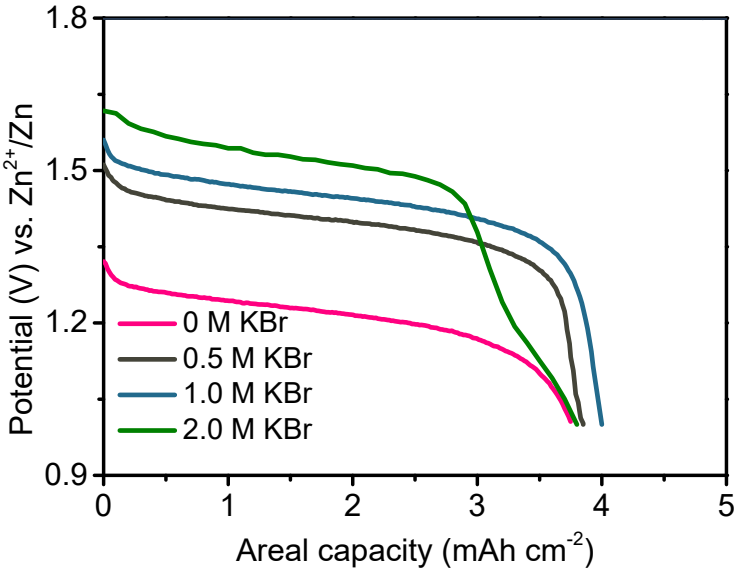

Figure S4. Discharge profiles of the Zn-MnO_2 batteries with different concentrations of KBr additives in the electrolytes with a discharge current density of 5 mA cm^{-2}.

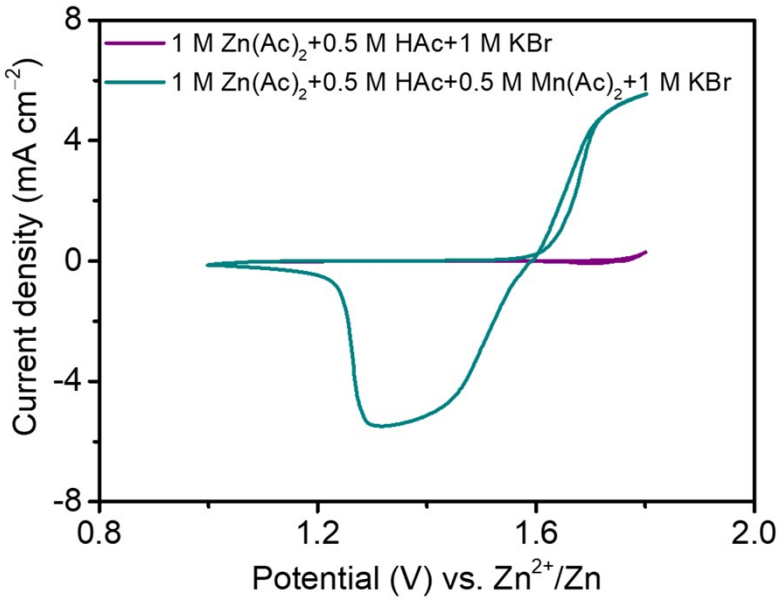

Figure S5. CV curves of cells with different electrolytes (1 M $Zn(Ac)_2$+0.5 M HAc +1M KBr and 1 M $Zn(Ac)_2$+0.5 M HAc+1 M KBr+0.5 M $Mn(Ac)_2$) at a scan rate of 0.5 mV s^{-1}.

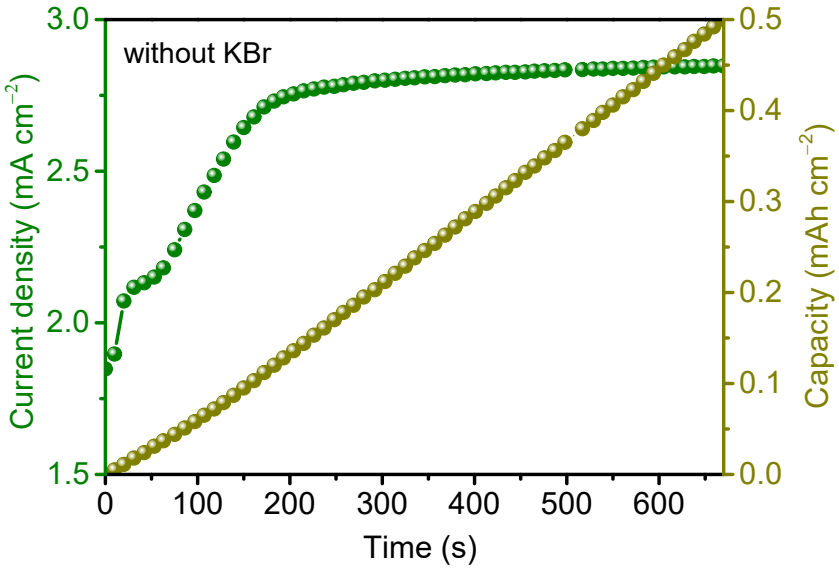

Figure S6. Charging behavior of the Zn-MnO_2 batteries with KBr-free additive electrolyte.

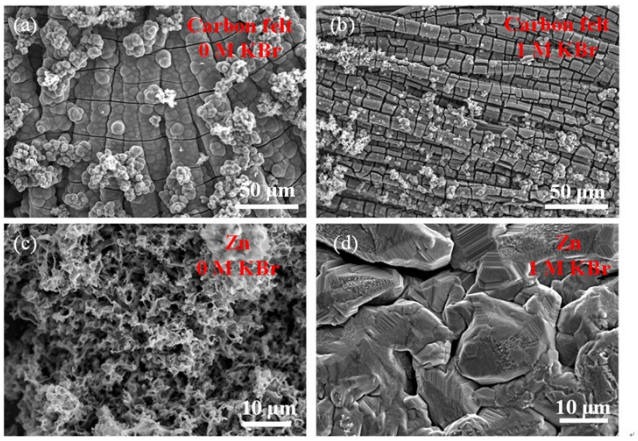

Figure S7. SEM images of carbon felt (a-b) and Zn electrodes (c-d) after charged at 1.8 V to an areal capacity of 10 mAh cm^{-2} in the electrolytes with and without 1.0 M KBr additive.

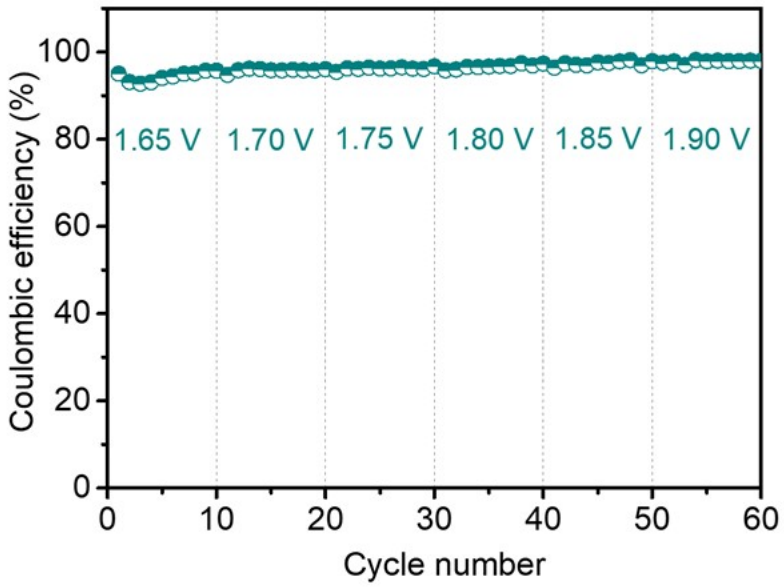

Figure S8. The cycling performance of the Zn-MnO_2 cell with 1 M KBr additive under different charging voltages from 1.65–1.90 V with a constant charging capacity of 1 mAh cm^{-2} and discharge current density of 5 mA cm^{-2}.

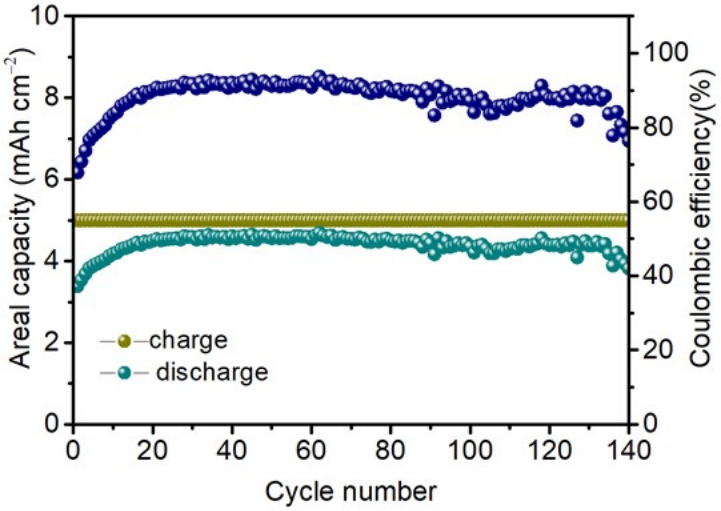

Figure S9. Cycling performance of the Zn-MnO_2 cell with 1 M KBr additive with a charging capacity of 5 mAh cm^{-2} and a discharge current density of 5 mA cm^{-2}.

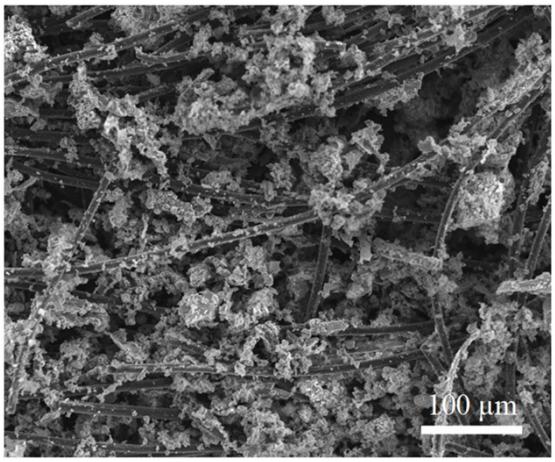

Figure S10. SEM image of carbon felt substrate after 1000 cycles in the electrolyte without KBr additive with a deposited capacity of 0.5 mAh cm^{-2} and a discharge current density of 5 mA cm^{-2}.

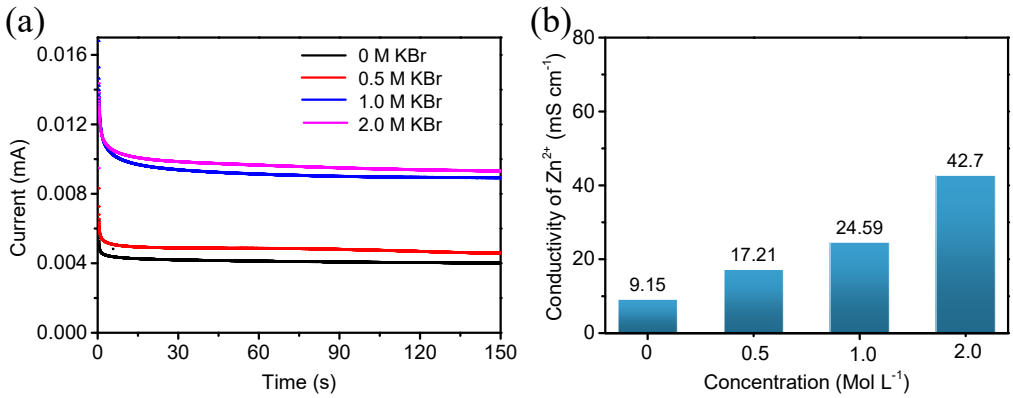

Figure S11. (a) Chronoamperometry curves of Zn symmetric cell and (b) Conductivity of Zn^{2+} in the electrolytes with different concentrations of KBr additive.

Table S1. The electrolyte structural feature and the binding energy of the Zn^{2+} and Mn^{2+} cations within different solvation sheaths (H_2O, Ac^- and Br^-).

Cations and ligands	Optimized structure	Binding energy (eV)	Cations and ligands	Optimized structure	Binding energy (eV)
$Zn+H_2O$		-4.8	$Mn+H_2O$		-3.8
$Zn+2H_2O$		-8.8	$Mn+2H_2O$	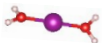	-6.9
$Zn+3H_2O$		-10.8	$Mn+3H_2O$		-8.6
$Zn+4H_2O$		-12.1	$Mn+4H_2O$		-9.3
$Zn+5H_2O$		-13.0	$Mn+5H_2O$		-10.0
$Zn+6H_2O$		-13.4	$Mn+6H_2O$		-9.9
$Zn+Ac^-$		-10.7	$Mn+Ac^-$	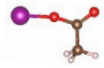	-8.3
$Zn+2Ac^-$	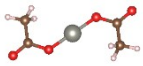	-15.8	$Mn+2Ac^-$	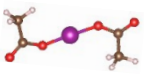	-13.4
$Zn+Br^-$		-10.3	$Mn+Br^-$		-8.4
$Zn+2Br^-$		-15.6	$Mn+2Br^-$	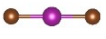	-12.7
$Zn+3Br^-$	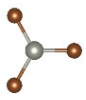	-17.0	$Mn+3Br^-$		-14.4
$Zn+4Br^-$	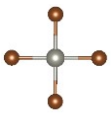	-16.1	$Mn+4Br^-$	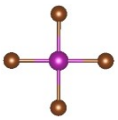	-13.7